

Enhanced Hepatic Uptake and Bioactivity of Type $\alpha 1(I)$ Collagen Gene Promoter-Specific Triplex-Forming Oligonucleotides after Conjugation with Cholesterol

Kun Cheng, Zhaoyang Ye, Ramareddy V. Guntaka, and Ram I. Mahato

Departments of Pharmaceutical (K.C., Z.Y., R.I.M.) and Molecular (R.V.G.) Sciences, University of Tennessee Health Science Center, Memphis, Tennessee

Received December 20, 2005; accepted January 30, 2006

ABSTRACT

A triplex-forming oligonucleotide (TFO) specific for type $\alpha 1(I)$ collagen promoter is a promising candidate for treating liver fibrosis. Earlier, we determined the pharmacokinetics and bio-distribution of TFO after systemic administration into normal and fibrotic rats. In this study, we conjugated cholesterol to the 3' end of the TFO via a disulfide bond and determined its cellular and nuclear uptake and bioactivity using HSC-T6 cell lines in vitro, followed by biodistribution at whole-body, organ (liver), and subcellular levels. Conjugation with cholesterol had little effect on the triplex-forming ability of the TFO with target duplex DNA, and the cellular uptake of ^{33}P -TFO-cholesterol (Chol) increased by 2- to approximately 4-fold. Real-time reverse transcriptase-polymerase chain reaction analysis after

transfection of HSC-T6 cells with TFO-Chol or TFO indicated that TFO-Chol had higher inhibition on type $\alpha 1(I)$ collagen primary transcript than naked TFO at low concentration (200 nM) but showed similar inhibition at higher concentration (500 and 1000 nM). There was increase in the inhibition on primary transcript with transfection time. The hepatic uptake of ^{33}P -TFO-Chol after systemic administration was 72.22% of the dose compared with 45.8% of ^{33}P -TFO. There was significant increase in the uptake of ^{33}P -TFO-Chol by hepatic stellate cells and hepatocytes. More importantly, the nuclear uptake of TFO-Chol was higher than TFO in cell culture system and in vivo studies. In conclusion, TFO-Chol is a potential antifibrotic agent.

Liver fibrosis is characterized by disproportionate accumulation of extracellular matrix components, especially types I and III fibrillar collagens. It results from chronic injury as a result of hepatitis B and C, viral infection, excessive alcohol ingestion, nonalcoholic steatohepatitis, and iron overload (Brenner et al., 1994). Liver fibrosis culminates in liver cirrhosis, the end stage leading to liver failure. Hence, a potent antifibrotic therapy is in an urgent need to slow or reverse liver fibrosis.

Because liver fibrosis is due to the overproduction of type I collagen by liver fibrogenic cells, inhibition of transcription of type $\alpha 1(I)$ collagen gene is expected to prevent fibrosis. Mammalian $\alpha 1(I)$ collagen gene promoter contains two contiguous 30-bp polypurine tracts C1 and C2, located at -141 to -170

and -171 to -200 upstream from the transcription start site (Joseph et al., 1997). We have previously shown that 18-, 25-, and 30-mer antiparallel phosphorothioate (APS) TFOs specific for C1 tract form triplexes efficiently and inhibit transcription in cultured fibroblasts (Joseph et al., 1997; Nakanishi et al., 1998).

Hepatic stellate cells (HSCs; also known as vitamin A-storing cells, fat-storing cells, Ito cells, and lipocytes) residing in the perisinusoidal space of Disse in the liver, are the main producers of type $\alpha 1(I)$ collagen and other components of extracellular matrix in both normal and fibrotic livers (Inagaki et al., 1995; Friedman, 2000). Hepatic myofibroblasts are another source of fibrogenic cells that derive from fibroblasts of the connective tissues, perivascular fibroblasts of portal and central veins, and periductular fibroblasts in close contact with bile duct epithelial cells (Knittel et al., 1999; Bedossa and Paradis, 2003). Excessive collagen production in the liver can be inhibited by triplex formation with type $\alpha 1(I)$ collagen gene promoter. Therefore, we recently determined

This work was supported by National Institutes of Health Grants R01 DK064633 and USPHS 47379.

Article, publication date, and citation information can be found at <http://jpet.aspetjournals.org>.
doi:10.1124/jpet.105.100347.

ABBREVIATIONS: APS, antiparallel phosphorothioate; TFO, triplex-forming oligonucleotide; bp, base pair(s); HSC, hepatic stellate cell; ODN, oligodeoxynucleotide; Chol, cholesterol; ESI, electrospray ionization; MS, mass spectrometry; DTT, dithiothreitol; HPLC, high-performance liquid chromatography; 3-HPA, 3-hydroxypicolinic acid; MALDI-TOF, matrix-assisted laser desorption ionization/time of flight; T4-PNK, T4 polynucleotide kinase; PBS, phosphate-buffered saline; FBS, fetal bovine serum; DMEM, Dulbecco's modified Eagle's medium; PCR, polymerase chain reaction; DMN, dimethylnitrosamine.

the pharmacokinetics and biodistribution of the ^{33}P -labeled 25-mer APS TFO after systemic administration into normal and liver fibrotic rats (Cheng et al., 2005). For enhanced delivery of the TFO to liver fibrogenic cells, we conjugated mannose 6-phosphate-bovine serum albumin to the TFO via a disulfide bond (Ye et al., 2005).

Because ODNs are polyanions and do not readily penetrate biological membranes, various strategies have been developed to increase their cellular uptake. Complex formation with cationic lipids or polycations (such as polyethylenimine) is presently commonly applied to facilitate their uptake by cells in culture, but it is not very suited for use in vivo (Juliano et al., 1999; Akhtar et al., 2000). An approach that was found to be effective, both in vitro and in vivo, is conjugation of ODNs with cholesterol. Conjugation of ODNs to hydrophobic compounds such as cholesterol, alkyl chain, or lipid have been shown to have higher cellular uptake than their unconjugated counterparts (Zhang et al., 1997; Okamoto et al., 1999; Bijsterbosch et al., 2000, 2001, 2002; Holasova et al., 2005). Improved efficacy of cholesterol conjugated ODNs was explained by the higher cellular uptake because the cholesterol conjugation increases hydrophobicity and cellular association (Bijsterbosch et al., 2000). Therefore, in the present study, we conjugated cholesterol to the 3' terminal of TFO via a disulfide bond to maximize TFO delivery to the liver cells, including HSCs. In vitro cellular uptake and bioactivity of TFO-Chol were measured and compared with unmodified TFO. We then determined the biodistribution of ^{33}P -TFO-Chol at whole-body, organ (liver), cellular, and subcellular levels after systemic administration.

Materials and Methods

Materials. The 25-mer APS TFO (5'-GGGA AGG AAA GGG AGG AGG GGG GAG-3') was purchased from The Midland Certified Reagent Company Inc. (Midland, TX), and TFO modified with a sulfhydryl group at the 3' end was purchased from Invitrogen Corporation (Carlsbad, CA). $[\gamma\text{-}^{33}\text{P}]\text{ATP}$ was obtained from MP Biomedicals (Irvine, CA), and T4 polynucleotide kinase was purchased from New England Biolabs (Beverly, MA). Bis-(5-nitro-2-pyridyl)-disulfide, thiocholesterol, triethylamine, 3-hydroxypicolinic acid, ammonium citrate, pronase, and Nuclei PURE Prep Nuclei Isolation Kit were purchased from Sigma-Aldrich (St. Louis, MO). Silica gel was purchased from Merck (Milwaukee, WI), and Bio-Gel P-6DG gel was

purchased from Bio-Rad Laboratories (Hercules, CA). Soluene-350 (tissue solubilizer) and Hionic-Fluor (scintillation fluid) were purchased from Perkin Elmer (Boston, MA). Isoflurane was obtained from Baxter Health Corporation (Deerfield, IL). Type IV collagenase was purchased from Worthington Biochemical Corporation (Lakewood, NJ). Nycodenz AG was obtained from Greiner Bio-One Inc. (Longwood, FL). PE-60 polyethylene tube was purchased from Becton Dickinson and Company (Sparks, MD), and heparin solution was procured from American Pharmaceutical Partners, Inc. (Los Angeles, CA).

Synthesis of 2-(5'-Nitropyridyl)-3-Cholesterol Disulfide. Synthesis scheme of TFO-Chol is shown in Fig. 1. Thiocholesterol (100 mg, 0.25 mmol) and bis-(5-nitro-2-pyridyl)-disulfide (120 mg, 0.4 mmol) were dissolved in 5 ml of pyridine and stirred at room temperature for 2 h (Alefelder et al., 1998). The solvent was removed and reconstituted with 50 ml of CH_2Cl_2 , followed by extraction with 25 ml of saturated NaHCO_3 , 30 ml of NaOH (1 N), and 40 ml of distilled water. The organic phase was dehydrated with Na_2SO_4 and evaporated using a rotatory evaporator. The product was dissolved in 10% (v/v) of CH_2Cl_2 in hexane and separated on silica gel with a linear gradient of CH_2Cl_2 in hexane from 10 to 40% (v/v), with 70% yield. The product, 2-(5'-nitropyridyl)-3-cholesterol disulfide, was characterized by electrospray ionization (ESI)-mass spectrometry (MS) and ^1H NMR.

Conjugation of Cholesterol to TFO. TFO modified with a sulfhydryl group at the 3' end (500 nmol) was treated with 0.2 M dithiothreitol (DTT) in 1500 μl of 0.1 M, pH 9.0, glycine buffer containing 0.1 M NaCl for 3 h at room temperature to generate a 3'-thiol functional group. Excess DTT was removed by extraction with ethyl acetate (4×1 ml), and TFO was precipitated by adding 3 volumes of ethanol after the addition of sodium acetate (NaOAc) to 0.3 M. The mixture was kept at -30°C overnight and centrifuged at 12,000g for 30 min at 4°C . Five milligrams of TFO with 3'-thiol functional group was dissolved in 600 μl of boric acid/borax buffer (pH 8.0, 60 mM). Ten milligrams of 2-(5'-nitropyridyl)-3-cholesterol disulfide was added, followed by 1500 μl of dimethylformamide. The mixture was incubated with stirring under N_2 protection at 40°C for 24 h.

TFO-Chol was purified by HPLC (Hewlett Packard Series 1000; Hewlett Packard Instrument Corp., Palo Alto, CA) on an XTerra MS C_{18} 2.5- μm , 4.6×50 -mm column (Waters Corporation, Milford, MA) using a 5 to 100% acetonitrile gradient in 0.1 M triethylammonium acetate buffer, pH 7.0. Flow rate was 1 ml/min, and column temperature was 60°C . Elution time for TFO-Chol was approximately 17 min, and the yield was above 90%.

3-Hydroxypicolinic acid (3-HPA) in ammonium citrate was used as

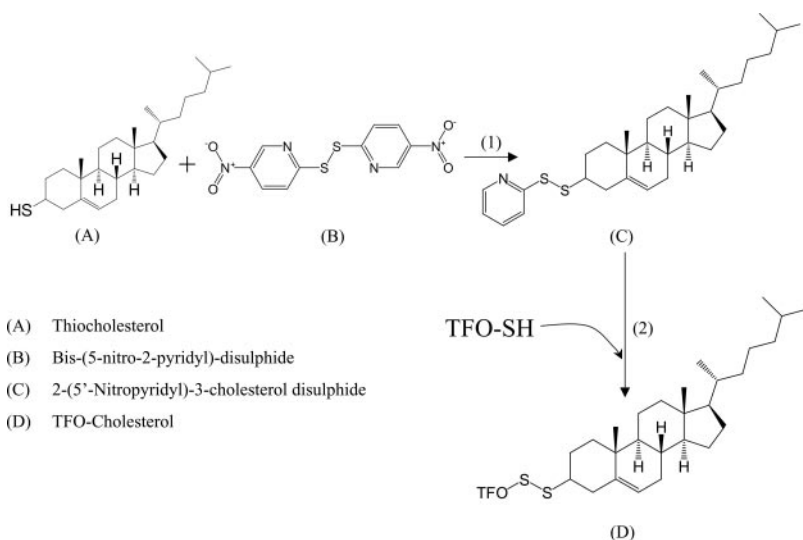


Fig. 1. Synthesis of TFO-Chol. Reagent and conditions: 1, 5 ml of pyridine, stirring at room temperature for 2 h; and 2, 1500 μl of dimethylformamide, stirring under N_2 protection at 40°C for 24 h.

a matrix to determine the mol. wt. of TFO-Chol using matrix-assisted laser desorption ionization/time of flight (MALDI-TOF; Voyager-DE RP; Applied Biosystems, Foster City, CA) mass spectrometer. Saturated solution of 3-HPA was prepared in 50 mM diammonium citrate solution containing 25% (v/v) acetonitrile. The mixture of TFO-Chol and 3-HPA (2 μ l) was spotted on the stainless steel probe tip and left to dry in the dark before MALDI-TOF analysis. MALDI-TOF spectra were operated in the linear, negative, delayed extraction mode. MALDI-TOF conditions were: accelerating potential, 22,000 V; guide wire, 0.12% of accelerating voltage; grid voltage, 95.4% of accelerating voltage; and delay extraction time, 600 ns.

Labeling of TFO. The 25-mer APS TFO or TFO-Chol was labeled by adding γ - ^{33}P to the 5' end using [γ - ^{33}P]ATP and T4 polynucleotide kinase (T4-PNK) using the manufacturer's protocol. Briefly, 1 μ g of TFO or TFO-Chol was mixed with 5 μ l of T4-PNK buffer, 2 μ l of T4-PNK, and 4 μ l of [γ - ^{33}P]ATP. The reaction mixture was incubated at 37°C for 60 min, followed by incubation at 70°C for 10 min to stop the reaction. Unincorporated [γ - ^{33}P]ATP was removed from radiolabeled TFO by size exclusion chromatography with Bio-Gel P-6DG gel (Bio-Rad Laboratories). Radioactivity was measured on a TRI-CARB 2000 liquid scintillation analyzer (PACKARD Instrument Company, Meriden, CT). The incorporation efficiency of the purified ^{33}P -TFO was determined by trichloroacetic acid precipitation method, and the value was more than 95%. The specific activity of ^{33}P -TFO was approximately 5×10^5 to approximately 10×10^5 cpm/ μ g.

Triplex Formation of TFO with Type α 1(1) Collagen Promoter. Double-strand oligodeoxyribonucleotides [corresponding to -168 to -139 of rat type α 1(1) collagen promoter] were prepared using equal amounts of complementary single strands (P1, 5'-CCT TTC CCT TCC TTT CC TCC TCC CCC CTC-3'; and P2, 5'-GAG GGG GGA GGA GGG AAA GGA AGG GAA AGG-3') in the presence of 0.25 M NaCl. The mixture was heated at 80°C for 5 min, incubated at 55°C for 30 min, 42°C for 30 min, and then at room temperature for 30 min. Triplex formation was initiated by mixing of DTT (100 mM)-treated ^{33}P -TFO-Chol with double-stranded oligodeoxyribonucleotide in a binding buffer containing 20 mM Tris-HCl, pH 7.4, and 20 mM MgCl_2 . Samples were incubated at 37°C for 3 h and analyzed on a 15% polyacrylamide gel in a buffer containing 89 mM Tris, 89 mM boric acid, pH 7.5, and 20 mM MgCl_2 for 3 h at 80 V at 4°C. Gel was visualized by autoradiography.

In Vitro Cellular and Subcellular Distribution of TFO-Chol. Immortalized rat liver hepatic stellate cell lines (HSC-T6) were plated at a density of 5×10^5 cells in a six-well plate at 12 h before transfection. After washing with PBS, 0.5, 1, 2.5, and 5 μ g of TFO or TFO-Chol mixed with ^{33}P -TFO or ^{33}P -TFO-Chol was added separately into cells with 0.6 ml of FBS-free DMEM. After incubation for 2 h, 1.4 ml of DMEM (14% FBS) was added and incubated for an additional 2 h. Cells were then washed two times with PBS, trypsinized, and 90% of the harvested cells were digested with Soluene-350 overnight. Hionic-Fluor was added, and the radioactivity was determined using a liquid scintillation counter. Ten percent of the harvested cells was used for protein content assay to normalize the cellular uptake results.

To determine the effect of cholesterol conjugation on the cytosolic and nuclear uptake of the TFO, HSC-T6 cells were incubated with ^{33}P -TFO-Chol at 37°C for 4 and 10 h, and cells were harvested and treated with Nuclei EZ lysis buffer (Sigma-Aldrich). The nuclei were then isolated using a NUC-101 kit as per the supplier's protocol (Sigma-Aldrich). The purity and number of isolated nuclei were determined under microscopy after dilution with trypan blue solution. Isolated nuclei were digested, and radioactivity was determined as described above.

In Vitro Bioactivity of TFO-Chol. HSC-T6 cells were plated at a density of 8×10^5 cells in six-well plates 12 h before transfection. TFO and TFO-Chol were diluted in 200 μ l of Opti-MEM I medium (Invitrogen) for 20 min at room temperature before transfection. The transfection mixture was then added to each plate with 1.3 ml of

FBS-free DMEM at concentration of 250, 500, and 1000 nM after washing cells with PBS. After 24 h of incubation, 0.5 ml of DMEM (10% FBS) was added and incubated for another 24 h.

Cells were collected and total RNA was isolated using RNA STAT 60 reagent (Ambion RNA Diagnostics, Austin, TX). Total RNA (1 μ g) was treated with DNase I (Sigma-Aldrich) and then converted to cDNA using MultiScribe Reverse Transcriptase Reagent and random hexamers (Applied Biosystems, Inc.). One hundred nanograms of the cDNA was amplified by real-time PCR using SYBR Green-1 dye universal master mix on ABI Prism 7700 Sequence Detection System (Applied Biosystems, Inc.). The forward and reverse primers specific for α 1(I) collagen mRNA were 5'-TGGTCCCAAAGTTCTC-CTGGT-3' and the reverse primer 5'-TTAGGTCCAGGAATC-CCATCACA-3', respectively. The forward primer specific for α 1(I) collagen primary mRNA was 5'-CCAGCCGCAAAGAGTCTACAT-GTC-3', and the reverse primer was 5'-TCACCTTCTCATCCCTC-CTAA-3'. The PCR product is 234 bp. Primer (forward, 5'-GTCTGT-GATGCCCTTAGATG-3'; and reverse, 5'-AGCTTATGACCCGCA-CTTAC-3') specific for 18S ribosomal RNA was used as internal control for real-time PCR. To confirm PCR specificity, the PCR products were subjected to a melting curve analysis and agarose gel electrophoresis. The comparative threshold method (Pfaffl, 2001) was used to calculate the relative amount of primary transcripts of TFO-treated sample to the untreated samples.

Biodistribution of TFO-Chol. The animal protocol was approved by the Animal Care and Use Committee (Department of Comparative Medicine, University of Tennessee Health Science Center, Memphis, TN). Male Sprague-Dawley rats (Harlan Co., San Diego, CA) weighing 180 g were used in this study, and four rats were used for each time point. Unlabeled and ^{33}P -TFO-Chol were mixed in saline to give a final concentration of 0.1 mg/ml and specific activity of 1×10^6 cpm/ml. Rats were anesthetized by inhalation of isoflurane, and ^{33}P -TFO-Chol was injected via tail vein at a dose of 0.21 mg/kg body weight. At various time points, 0.5 ml of blood was collected by cardiac puncture in heparinized tubes, and urine was collected directly from the bladder using a 0.26-gauge needle syringe. The animals were then sacrificed, and major tissues (liver, kidney, spleen, heart, lung, and muscle) were collected, washed, blotted dry, weighed, and stored at -80°C. The radioactivity of urine sample was counted directly after adding 10 ml of scintillation fluid. One hundred fifty microliters of plasma and 150 mg of each tissue were incubated with 2 ml of tissue solubilizer for 3 h at 55°C and overnight at room temperature. Three hundred fifty microliters of H_2O_2 was added and incubated at 55°C for another 30 min. Ten milliliters of scintillation fluid was added to each sample, and the radioactivity was counted using a liquid scintillation counter.

Induction of Liver Fibrosis. Liver fibrosis was induced by i.p. injections of dimethylnitrosamine (DMN) into rats at a dose of 1 ml (1% in saline)/kg body weight. This is a well established animal model for liver fibrosis that has similar pathophysiological properties to those of human liver fibrosis (Jenkins et al., 1985; Jezequel et al., 1987). Injections were given on the first 3 consecutive days of each week over a 3-week period. After the DMN injection for 3 weeks, three rats were killed for examination of liver fibrosis development and measurement of hydroxyproline content as described by Jamall et al. (1981). After 3 weeks of treatment, rats were used for biodistribution studies.

Hepatic Cellular Distribution. After i.v. injection of ^{33}P -TFO and ^{33}P -TFO, rat liver was perfused as described before (Cheng et al., 2005). Briefly, rats (200–250 g) were anesthetized, and heparin (100 IU) was injected via tail vein, the abdomen was opened, and the portal vein was cannulated with PE-60 polyethylene tube. The liver was preperfused with 2 ml of diluted heparin solution, then with 200 ml of $\text{Ca}^{2+}/\text{Mg}^{2+}$ -free Hank's balanced salt solution, and finally with Hanks' balanced salt solution containing 0.05% type IV collagenase and 0.1% pronase for an additional 250 ml. All the perfusion solutions were incubated at 37°C. After perfusion, different liver cell

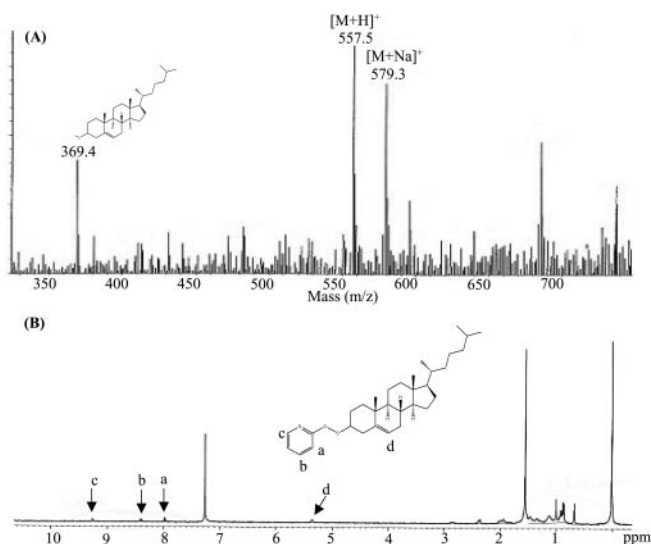


Fig. 2. Characterization of intermediate products with ESI-MS (A) and ^1H NMR (B). ESI mass spectra were obtained in 40% (v/v) of CH_2Cl_2 in hexane on an ESQUIRE-LC Ion Trap liquid chromatography/MS system. For ^1H NMR, samples were dissolved in CDCl_3 , and the spectra were recorded on a Bruker ARX-300 MHz spectrometer (AnaLtech Inc., Newark, DE) at 25°C.

types were separated by Nycodenz gradient, and radioactivity was measured as described before (Cheng et al., 2005).

Hepatic Subcellular Distribution of TFO-Chol. To determine the subcellular distribution of TFO-Chol, the liver was collected at 2 and 4 h postinjection of ^{33}P -TFO-Chol into the rats via tail vein at a dose of 0.2 mg/kg. One gram of the liver was used for isolation of nuclei using a NUC-201 kit (Sigma-Aldrich) and determination of radioactivity as described above. The percentage of nuclear uptake of the TFO in the liver was calculated as $\text{TFO}_{\text{nuclei}}/\text{TFO}_{\text{liver}}$.

Statistical Analysis. Data were expressed as the mean \pm S.D. Difference between any two groups was determined by analysis of variance. $P < 0.05$ was considered statistically significantly.

Results

To enhance the cellular uptake and nuclear translocation of the TFO, we conjugated cholesterol to the 3' end of the TFO via a disulfide bond. TFO-Chol was then characterized

in terms of mol. wt., chemical structure, and in vitro cellular and nuclear uptake in HSC-T6 cell lines. This was followed by biodistribution at whole-body, organ (liver), and subcellular levels after i.v. injection into rats.

Synthesis and Characterization of TFO-Chol. As shown in Fig. 2, ESI-MS peaks (positive ion mode) of the intermediate product, 2-(5'-nitropyridyl)-3-cholesterol disulfide, were 557.5 $[\text{M}+\text{H}]^+$ and 579.5 $[\text{M}+\text{Na}]^+$, whereas peak 369.4 is for cholesterol, which was obtained after breakage of the disulfide bond of this product. The peak 685.5 comes from the impurities in the solvent. Figure 2B shows the ^1H NMR (CDCl_3) spectra of 2-(5'-nitropyridyl)-3-cholesterol disulfide.

Conjugation with cholesterol increased the hydrophobicity of the TFO, leading to significant increase in the elution time of TFO-Chol when purified using HPLC with XTerra MS C_{18} (2.5 μm , 4.6 \times 50 mm) column (Fig. 3A). Based on the peak area of TFO-Chol and unmodified TFO, the yield of the reaction was as high as 90%. The mol. wt. of TFO-Chol was determined using a MALDI-TOF mass spectrophotometer. Native TFO showed two mass peaks, $[\text{M}-\text{H}]^-$ ion (m/z 8378.85) and $[\text{M}-2\text{H}]^{2-}$ ion (m/z 4195.01) (Fig. 3B), whereas TFO-Chol showed two mass peaks, $[\text{M}-\text{H}]^-$ ion (m/z 8945.15) and $[\text{M}-2\text{H}]^{2-}$ ion (m/z 4480.89) (Fig. 3C). The mol. wt. difference between TFO-Chol and native TFO is 567, suggesting cholesterol conjugation to the TFO via a disulfide bond.

Effect of Cholesterol on Triplex Formation. Disulfide linkage between TFO and cholesterol is expected to be cleaved inside the cells by disulfide exchange with intracellular thiols or by the action of redox enzyme (Feener et al., 1990; Oberhauser and Wagner, 1992; Wang et al., 1998). Therefore, TFO-Chol was treated with DTT and incubated with the target duplex DNA to form triplex at physiological conditions and then was determined using gel shift assay. As shown in Fig. 4, ^{33}P -TFO-Chol formed the triplex same as ^{33}P -TFO. In addition, the triplex formation is dose-dependent, which is in accordance with our previous studies (Joseph et al., 1997).

In Vitro Cellular Uptake and Subcellular Distribution of TFO-Chol. To confirm that hydrophobization of the TFO enhances its cellular internization, we determined the

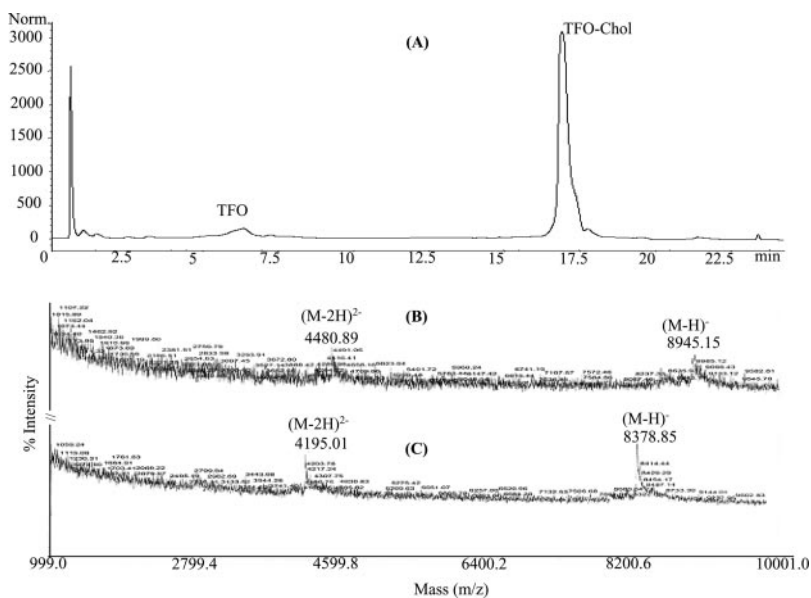


Fig. 3. Purification of TFO-Chol with HPLC (A) and determination of TFO-Chol mol. wt. with MALDI-TOF spectrophotometry (B and C). The mol. wt. of TFO-Chol was determined using MALDI-TOF (Voyager-DE RP; Applied Biosystems). 3-HPA in ammonium citrate was used in as matrix.

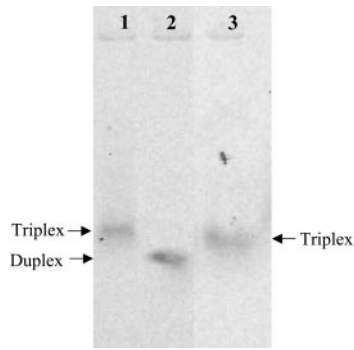


Fig. 4. Triplex formation of TFO-Chol with type $\alpha 1(I)$ collagen promoter. TFO-Chol was mixed with double-stranded oligonucleotides corresponding to -168 to -139 of rat type $\alpha 1(I)$ collagen promoter, and samples were applied on 15% native polyacrylamide gel electrophoresis at 4°C in 89 mM Tris-borate buffer, containing $MgCl_2$ (20 nM) for 3 h. Lane 1, ^{33}P -duplex DNA incubated with TFO for 3 h at 37°C; lane 2, ^{33}P -duplex DNA; lane 3, TFO-Chol incubated with DTT for 2 h at 37°C, followed with incubation with ^{33}P -duplex DNA for 3 h at 37°C.

cellular uptake of ^{33}P -TFO-Chol in HSC-T6 cells at 2 h postincubation at 37°C. As shown in Fig. 5, ^{33}P -TFO-Chol has 2- to 4-fold higher cellular uptake compared with ^{33}P -TFO at different doses ranging from 0.5 to 5 μg .

To inhibit the transcription of type $\alpha 1(I)$ collagen, TFO must enter the nucleus and form triple helices with the genomic DNA. Fractionation by sucrose gradient gave fairly pure and intact nuclei, with recovery of 40 to approximately 45% (data not shown). ^{33}P -TFO-Chol had higher nuclear uptake than that of ^{33}P -TFO. Compared with ^{33}P -TFO, the uptake of ^{33}P -TFO-Chol was 2-fold higher in the cytoplasm and 3-fold higher in the nucleus at 4 h of incubation with HSC-T6 cells at 37°C (Fig. 6). However, the difference was not significant at 10 h postincubation, indicating that conjugation of cholesterol to the TFO increases the rate of its cytosolic and nuclear uptake. Nevertheless, both the extent and rate of cellular and nuclear uptake of ^{33}P -TFO-Chol were higher at early time points.

In Vitro Bioactivity of TFO-Chol. To determine whether cholesterol conjugation to the TFO enhance the inhibitory effect of the TFO on collagen transcription, HSC-T6 cell lines were incubated with TFO or TFO-Chol at different time and different doses, followed by extraction of total RNA and quantified with real-time PCR. As Fig. 7A showed, both

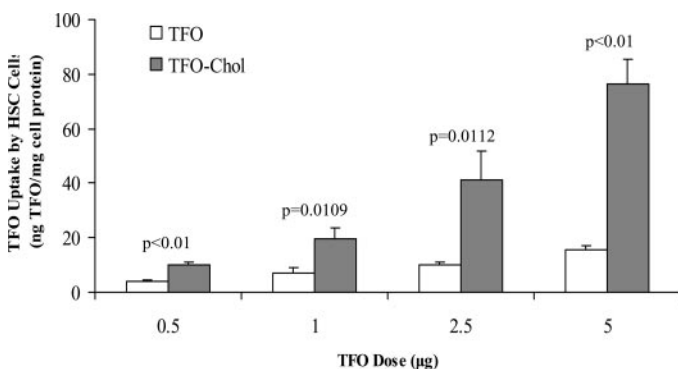


Fig. 5. Cellular uptake of ^{33}P -TFO-Chol and ^{33}P -TFO in cultured HSC-T6 Cells after incubation for 4 h at doses of 0.5, 1, 2.5, and 5 μg of TFO per 5×10^5 HSC-T6 cells. Radioactivity was determined using a liquid scintillation counter after digestion of trypsinized cells with Soluene-350. Results were normalized with protein content. Data are represented as the mean \pm S.D. ($n = 3$).

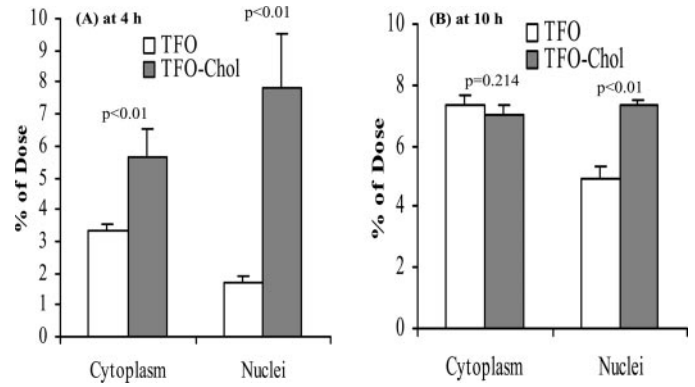


Fig. 6. Subcellular distribution of ^{33}P -TFO-Chol and ^{33}P -TFO in cultured HSC-T6 cells after incubation at 37°C for 4 and 10 h at a dose of 0.5 μg of TFO per 5×10^5 HSC-T6 cells. Radioactivity was determined using a liquid scintillation counter after digestion of isolated nuclei, cytoplasm, and cell membrane using NUC-101 kit (Sigma-Aldrich). Results are represented as the mean \pm S.D. ($n = 3$).

TFO and TFO-Chol exhibited specific inhibition of collagen primary transcript expression, and the inhibition increased with transfection time. At 48 h post-transfection, more than 80% of the primary transcripts were inhibited by both TFO and TFO-Chol. TFO-Chol showed higher inhibition than TFO at 6 h and 10 h transfection, whereas no difference was observed at 48 h transfection. Dose effect was also investigated at 200, 500, and 1000 nM (Fig. 7B). At 200 nM, TFO-Chol inhibited 50% of type $\alpha 1(I)$ collagen primary transcript,

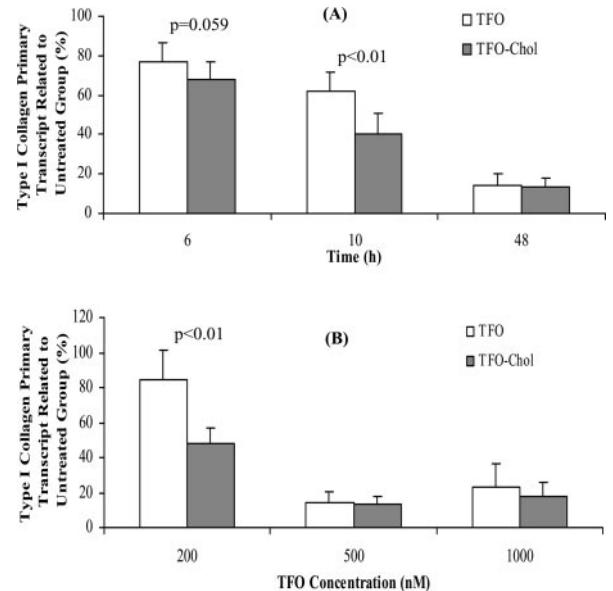


Fig. 7. Inhibition of type $\alpha 1(I)$ collagen gene transcription after incubation of HSC-T6 cells with TFO-Chol or TFO. A, effect of incubation time on transcription inhibition. B, effect of dose on transcription inhibition. To determine the effect of incubation time (A), HSCs were incubated with 500 nM TFO and TFO-Chol for 6, 10, and 48 h, followed by replacing with fresh culture medium. To determine the effect on dose on inhibition of type $\alpha 1(I)$ collagen transcription (B), various concentrations (200, 500, and 1000 nM) of TFO and TFO-Chol were used for transfection for 48 h. After transfection, cells were collected, and total RNA was isolated. Total RNA (1 μg) was converted to cDNA, and 100 ng of the extracted cDNA was amplified by real-time PCR using SYBR Green-1 dye universal master mix on ABI Prism 7700 Sequence Detection System. Primer pairs specific for the $\alpha 1(I)$ collagen primary mRNA are forward primer 5'-CCAGCCGCAAAAGAGTCTACATGTC-3' and the reverse primer 5'-TCACCTTCTCATCCTCCTAA-3'; the PCR product is 234 bp. Results are represented as the mean \pm S.D. ($n = 6$).

whereas TFO only inhibited 15%. At 500 and 1000 nM, TFO-Chol showed similar inhibition as TFO. These results indicated that the conjugation of cholesterol to the TFO not only improved the cellular uptake but also increased the bioactivity of the TFO for inhibiting transcription of type $\alpha 1(I)$ collagen. Melting curve analysis showed single clear peak for all PCR products (data not shown), indicating high purity of the amplification. This finding was in parallel with the higher cellular and nuclear uptake of TFO-Chol by HSC-T6 cells.

Biodistribution of TFO-Chol. After confirming the enhanced cellular and nuclear uptake and bioactivity of TFO-Chol in HSC-T6 cell lines, we next determined whether conjugation with cholesterol can increase TFO deposition to the liver after i.v. injection of ^{33}P -TFO-Chol into rats at a dose of 0.2 mg/kg at 30 min and 4 h. Figure 8 shows the time course of radioactivity in the plasma, urine, liver, kidney, lung, heart, and muscle. In the case of ^{33}P -TFO, 7.94% of the injected dose was found in the circulation at 30 min postinjection but decreased to approximately 0.78% at 4 h postinjection. In contrast, ^{33}P -TFO-Chol was rapidly cleared from the circulation with only 2.54 and 0.84% of radioactivity in the plasma at 30 min and 4 h postinjection, respectively. There was a significant increase in the accumulation of radioactivity in the liver. In the case of ^{33}P -TFO, almost 45.8% of the injected dose was detected in the liver at 30 min but decreased to 37.97% at 4 h postinjection. In contrast, approximately 72.22% of the injected dose of ^{33}P -TFO-Chol was detected in the liver at 30 min but decreased to 55.73% at 4 h postinjection.

Fibrosis results in scar formation and changes in the sub-endothelial space of Disse and sinusoids, which may affect the hepatic uptake of the TFO (Friedman, 2000). Our earlier work has showed significant decrease in the TFO uptake by the liver of fibrotic rats (Cheng et al., 2005). Therefore, we determined the biodistribution of ^{33}P -TFO-Chol at 30 and 60 min postsystemic administration in DMN-induced liver fibrotic rats. The hepatic uptake of ^{33}P -TFO-Chol decreased from 72 to 52%, whereas the plasma concentration increased from 2.54 to 9.4% at 30 min postinjection (Fig. 9). Likewise, at 60 min postinjection, the hepatic uptake of ^{33}P -TFO decreased from 60 to 53%, and the plasma concentration increased from 2.32 to 5.08% at 60 min postinjection (Fig. 9). In addition, compared with the normal rats, significant increase

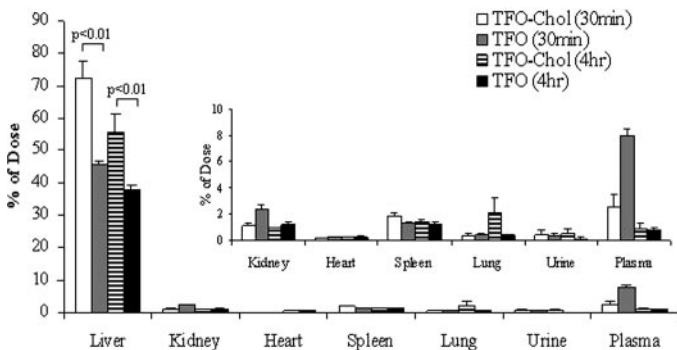


Fig. 8. Biodistribution of TFO-Chol after systematic administration of a mixture of ^{33}P -TFO-Chol and TFO or a mixture of ^{33}P -TFO and TFO at a dose of 0.2 mg/kg. At 30 min and 4 h after injection, blood was collected by cardiac puncture, and urine was collected from the bladder. The rats were sacrificed, tissues were collected, washed, and weighed, 150 mg of tissue was digested, and radioactivity was determined using a scintillation counter. Data are represented as the mean \pm S.D. ($n = 4$).

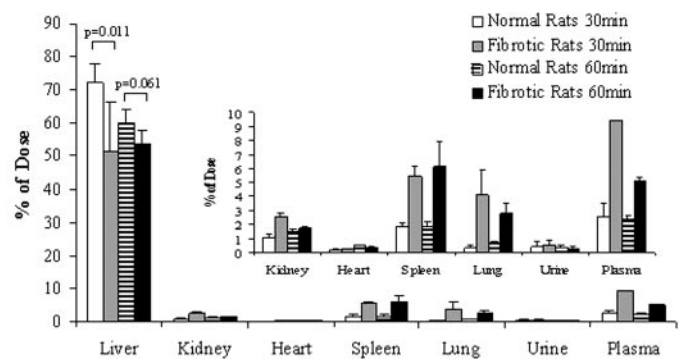


Fig. 9. Effect of liver fibrosis on biodistribution of TFO-Chol. At 30 min (A) and 4 h (B) after i.v. injection of ^{33}P -TFO-Chol into normal and DMN-induced fibrotic rats at a dose of 0.2 mg/kg, blood was collected by cardiac puncture, and urine was collected from the bladder. The rats were sacrificed, tissues were collected, washed, and weighed; 150 mg of tissue was digested, and radioactivity was determined using a scintillation counter. Data are represented as the mean \pm S.D. ($n = 4$).

in TFO concentration was also observed in the spleen, lung, and plasma in the liver fibrotic rats (Fig. 9).

Hepatic Cellular Distribution. To determine the intrahepatic distribution of TFO-Chol, the liver was perfused at 30 min postinjection of ^{33}P -TFO-Chol at a dose of 0.2 mg/kg, and different liver cells were isolated as described before (Cheng et al., 2005). As shown in Fig. 10, HSCs were the major site for the uptake of TFO-Chol in the liver (35.19% of the dose), whereas hepatocytes accounted for 25.42% of the dose, and Kupffer and endothelial cells accounted for 11.61% of the dose.

Hepatic Subcellular Localization. Nuclear translocation of TFO is vital for triplex formation with genomic DNA and consequent inhibition of collagen transcription. Although we demonstrated higher nuclear uptake of ^{33}P -TFO-Chol than that of ^{33}P -TFO in HSC-T6 cells, it was important to determine the nuclear uptake of ^{33}P -TFO-Chol in the rat liver after i.v. administration. Therefore, we determined the subcellular distribution ^{33}P -TFO-Chol in the cytoplasm and nuclear extracts after isolation of highly pure nuclei from the rat liver at 2 and 4 h postinjection of ^{33}P -TFO-Chol at a dose of 1 mg/kg. Recovery of nuclei was calculated to be 42 to 45% by comparing the number of isolated nuclei with the starting number. Figure 11A showed that the percentage of nuclear

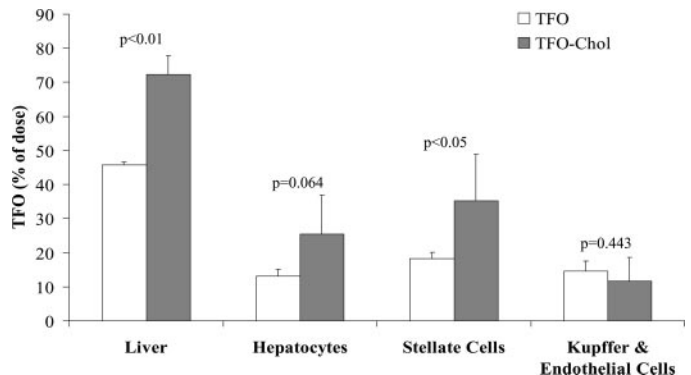


Fig. 10. Hepatic cellular localization of ^{33}P -TFO-Chol and ^{33}P -TFO after i.v. injection into rats at dose of 0.2 mg/kg. Different liver cells were isolated by in situ liver perfusion with a mixture of 0.05% collagenase and 0.1% pronase and fractionation on Nycodenz gradient. The amount of TFO-Chol found in each cell type is given as percentage of administered dose. Data are represented as the mean \pm S.D. ($n = 5$).

uptake of ^{33}P -TFO-Chol in the liver was similar to that of ^{33}P -TFO at 2 and 4 h but both increased with the incubation time from 2 to 4 h. However, the absolute amount of ^{33}P -TFO-Chol translocated to the liver nuclei at 4 h postsystemic administration was higher than that of ^{33}P -TFO by 50% (Fig. 11B). The above results indicate that the addition of cholesterol moiety to the TFO not only increased the nuclear uptake in the cell culture system but also increased the nuclear uptake in the liver after systemic administration of TFO-Chol.

Discussion

Hydrophobization of ODNs is known to facilitate their binding to cellular membranes, enhance their cellular uptake by endocytosis, and improve their stability (Godard et al., 1995). In addition, conjugation with cholesterol has been reported to enhance accumulation of ODNs and siRNA in the liver, resulting in their improved biological activity (Godard et al., 1995; Bijsterbosch et al., 2000; Manoharan, 2004). In this study, we conjugated cholesterol to type $\alpha 1(\text{I})$ collagen gene promoter-specific TFO at 3' end and characterized TFO-Chol in terms of triplex formation efficiency, cellular and subcellular uptake, bioactivity, tissue distribution, and hepatic cellular localization after systemic administration of ^{33}P -TFO-Chol in normal and fibrotic rats. TFO modified at the 3' end by a sulfhydryl group coupled to cholesterol-bearing activated thiol groups at a very high efficiency (>90%). The high yield of TFO-Chol provides a promising future for its therapeutic applications. Compared with 5' end modification, 3'-cholesterol conjugation of ODNs are much more stable in vivo (Crooke et al., 1996).

Cholesterol plays a pivotal role in regulating the properties of cell membranes. It occupies the space between the saturated hydrocarbon chains of sphingolipids in the cell membrane and makes the fluid membrane rigid (Simons and Ikonen, 2000). Cholesterol attached to the TFO may facilitate the anchoring of the conjugate to lipophilic cellular structure

(MacKellar et al., 1992) and prevent translocation to the nucleus where TFO needs to form triple helix with genomic DNA to function as an antigene (Boutorine and Kostina, 1993). In the present study, we conjugated cholesterol to the TFO via a disulfide bond that is known to be cleaved inside the cells with intracellular thiols or by the action of redox enzyme. As shown in Fig. 6, conjugation of cholesterol to the TFO did not prevent its translocation to the nucleus; instead, it provided a faster cellular and nuclear uptake of TFO compared with ^{33}P -TFO (Figs. 5 and 6). TFO-Chol had higher nuclear uptake than unmodified TFO at 4 h after incubation at 37°C (Fig. 6). Compared with ^{33}P -TFO, ^{33}P -TFO-Chol had rapid uptake and more uniform distribution in the cytoplasm and nucleus, which is in good agreement with the work of Alahari et al. (1996) and Holasova et al. (2005). Effective cellular uptake of ^{33}P -TFO-Chol in the absence of cationic lipids provides a promising antigene therapy for treating liver fibrosis because cationic liposomes and nanoparticles cannot be used for TFO delivery because of the disappearance of sinusoidal gap in the fibrotic liver.

TFO can function well only when it can form triplex with the genomic DNA in the nucleus of the target cells. Therefore, it is important to demonstrate not only the higher cellular uptake but also the higher nuclear uptake of ^{33}P -TFO-Chol. As shown in Fig. 6, ^{33}P -TFO-Chol has significantly higher nuclear translocation than TFO at 4 h postincubation, whereas after 10 h of incubation, the difference was relatively small. The same trend was found for cytoplasmic uptake of ^{33}P -TFO-Chol. In contrast, both nuclear and cytoplasmic uptake of TFO at 10 h was higher than that at 4 h. Conjugation of cholesterol to TFO provides a rapid cellular and nuclear uptake at early time points. The rapid uptake of cholesterol modified ODNs was also demonstrated by Krieg et al. (1993) and Holasova et al. (2005). The cholesterol-conjugated ODNs were believed to partition directly into the cell membrane, which contributed to rapid internalization of the ODN-Chol via adsorptive endocytosis.

Previously, we have reported that the TFO can form triplex with the type $\alpha 1(\text{I})$ collagen promoter sequence and inhibit chloramphenicol gene expression when we transfected fibroblasts with the plasmid DNA encoding this gene driven by the collagen promoter. In this study, we determined the inhibitory effect of TFO-Chol and TFO for type $\alpha 1(\text{I})$ collagen gene rather than on a reporter gene driven by the collagen promoter. Because the half-life of type $\alpha 1(\text{I})$ collagen mRNA is much longer in activated HSCs than in quiescent HSCs (Sato et al., 2003), it is difficult to detect the effect of TFO at the mRNA level in HSC-T6 cells. Therefore, we designed primers specific for type $\alpha 1(\text{I})$ collagen primary transcript to avoid this problem and demonstrated the inhibitory effect of TFO on type $\alpha 1(\text{I})$ collagen transcription. Both TFO-Chol and unmodified TFO inhibited type $\alpha 1(\text{I})$ collagen transcription after transfection with Lipofectamine (data not shown) or without any cationic liposomes. This is the first report to demonstrate direct inhibition of type $\alpha 1(\text{I})$ collagen transcription by the TFO using HSC-T6 cells.

Compared with the naked TFO, TFO-Chol exhibited somewhat higher levels of inhibition, especially at low concentrations and short transfection time (Fig. 7), which is in good agreement with the faster cellular uptake. Incubation time of TFO with cells also played an important role in the antigene efficacy (Fig. 7A). Both TFO-Chol and TFO exhibited signif-

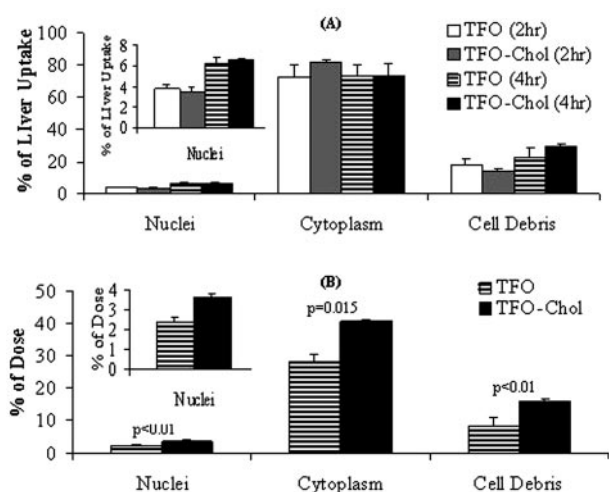


Fig. 11. Subcellular distribution of ^{33}P -TFO-Chol in the liver at 2 and 4 h after i.v. administration in rats at dose of 0.2 mg/kg. Nuclei were isolated from cytoplasm and cell debris using the sucrose gradient separation method. The purity and number of isolated nuclei were determined under microscopy by dilution in trypan blue solution. TFO distributions in the nuclei, cytoplasm, and cell debris are given as percentage of the total liver recovery (A) and percentage of the injected dose (B). Data are presented as the mean \pm S.D. ($n = 4$).

icantly higher transcription inhibition with increase in the incubation time. For 6- and 10-h incubation, TFO-Chol showed higher transcription inhibition than the TFO but no difference at 48 h postincubation. At low concentration (200 nM), TFO-Chol had a substantially higher antigene inhibitory efficacy than the TFO, but this difference was lost at higher concentration of 500 and 1000 nM. As Fig. 7B indicated, increasing concentration from 500 to 1000 nM did not increase the antigene inhibition efficacy for TFO-Chol and TFO. The same results were also observed by Alahari et al. (1996). These results suggest that cholesterol conjugation to the TFO increased the rapidity rather than the extent of the uptake in HSC-T6 cells. Therefore, after 48 h of incubation with HSC-T6 cells, TFO exhibited the cellular uptake and consequent antigene efficacy similar to those of TFO-Chol. These findings suggest that cholesterol conjugation not only enhanced the cellular and nuclear uptake of the TFO but also improved its bioactivity. In accordance with the work of Alahari et al. (1996), the experimental variation of TFO-Chol was less than that of the TFO in the bioactivity study, indicating uniformity in cellular and nuclear uptake.

After confirming higher cellular and nuclear uptake as well as bioactivity of TFO-Chol using HSC-T6 cell lines, we then determined its biodistribution and hepatic cellular and subcellular localization after tail vein injection in rats. As expected, there was significant increase in TFO-Chol accumulation in the liver of normal rats compared with free TFO (Fig. 8). This is in a good agreement with the work of Bijsterbosch et al. (2000, 2002), who also demonstrated enhanced liver accumulation of cholesterol-conjugated antisense ODNs. Furthermore, we determined the biodistribution of TFO-Chol in fibrotic rats since liver fibrosis resulted in lower liver uptake of the TFO in our previous study (Cheng et al., 2005), although the uptake of TFO-Chol by the fibrotic liver decreased compared with that by the normal liver (Fig. 9). However, the hepatic uptake of ^{33}P -TFO-Chol was higher than that of ^{33}P -TFO in both normal and fibrotic rats, providing an advantage for treating liver fibrosis.

We have previously reported that the hepatic uptake of TFO is mainly due to liver nonparenchymal cells (Cheng et al., 2005). The similar trend was observed for TFO-Chol, but with higher uptake. Compared with the unconjugated ^{33}P -TFO, uptake of ^{33}P -TFO-Chol by hepatocytes and HSCs increased approximately 2-fold, whereas the uptake by Kupffer and endothelial cells did not show significant increase (Fig. 10). Although HSCs and hepatocytes accumulated increased amount of ^{33}P -TFO-Chol, the concentration of ^{33}P -TFO-Chol in HSCs was much higher than in hepatocytes because HSCs constitute a much smaller cellular compartment than hepatocytes. Enhanced uptake of ^{33}P -TFO-Chol by HSCs is expected to result in improved therapeutic effect because these cells are the targets of TFO for antifibrotic effect. Our results are not fully in accordance with the work of Bijsterbosch et al. (2000, 2002), who also observed higher uptake of cholesterol conjugated ODN by endothelial cells, Kupffer cells, and hepatocytes. Because these authors did not isolate HSCs, thus the reported uptake of ODNs by Kupffer and endothelial cells may be an overestimate.

Because TFO-Chol has to enter the nucleus to inhibit transcription of type 1 collagen gene, we also determined the subcellular distribution of TFO-Chol in the cytoplasm and nuclear extracts after isolation of highly purified nuclei from

the liver after systemic administration of ^{33}P -TFO-Chol. As shown in Fig. 11A, for the TFO uptake by the liver cells, the same percentage was found in the nuclei for ^{33}P -TFO-Chol and ^{33}P -TFO. However, because ^{33}P -TFO-Chol has significantly higher liver uptake than ^{33}P -TFO, the total liver nuclear uptake of ^{33}P -TFO-Chol is higher than ^{33}P -TFO (Fig. 11B). This finding is in good agreement with the findings of Krieg et al. (1993), who used a confocal microscope to demonstrate higher cellular uptake of the ODNs after conjugation with cholesterol. In addition, these authors suggested the possible utility of ODN-Chol conjugates as gene transcription inhibitors via triplex formation.

What are the therapeutic implications of the present findings? Conjugation with cholesterol resulted in increased uptake by liver cells, in particular HSCs and hepatocytes. For liver-associated targets, conjugation of ODNs with cholesterol should therefore be beneficial. The rationale behind our TFO approach is to attack the final stage in the pathway leading to fibrosis because regardless of how fibrosis is induced, the ultimate is abnormal synthesis and accumulation of fibrillar collagens, especially type $\alpha 1(\text{I})$ and, therefore, is an ideal step to intervene. Because HSCs are the major cell type responsible for collagen synthesis, TFO-Chol is expected to increase the therapeutic effectiveness of the TFO for treating liver fibrosis. Increase in the uptake of ^{33}P -TFO-Chol by hepatocytes should not cause any problem because hepatocytes do not produce collagen.

In conclusion, cholesterol conjugation to the TFO enhanced its cellular uptake, nuclear translocation, and transcription inhibition of type $\alpha 1(\text{I})$ collagen in HSC-T6 cells in vitro and enhanced uptake by the liver and HSCs after systemic administration in both normal and fibrotic rats.

References

- Akhtar S, Hughes MD, Khan A, Bibby M, Hussain M, Nawaz Q, Double J, and Sayyed P (2000) The delivery of antisense therapeutics. *Adv Drug Deliv Rev* **44**:3-21.
- Alahari SK, Dean NM, Fisher MH, Delong R, Manoharan M, Tivel KL, and Juliano RL (1996) Inhibition of expression of the multidrug resistance-associated glycoprotein of phosphorothioate and 5' cholesterol-conjugated phosphorothioate antisense oligonucleotides. *Mol Pharmacol* **50**:808-819.
- Alefelder S, Patel BK, and Eckstein F (1998) Incorporation of terminal phosphorothioates into oligonucleotides. *Nucleic Acids Res* **26**:4983-4988.
- Bedossa P and Paradis V (2003) Approaches for treatment of liver fibrosis in chronic hepatitis C. *Clin Liver Dis* **7**:195-210.
- Bijsterbosch MK, Manoharan M, Dorland R, Van Veghel R, Biessen EA, and Van Berkel TJ (2002) bis-Cholesteryl-conjugated phosphorothioate oligodeoxynucleotides are highly selectively taken up by the liver. *J Pharmacol Exp Ther* **302**:619-626.
- Bijsterbosch MK, Manoharan M, Dorland R, Waarlo IH, Biessen EA, and van Berkel TJ (2001) Delivery of cholesteryl-conjugated phosphorothioate oligodeoxynucleotides to Kupffer cells by lactosylated low-density lipoprotein. *Biochem Pharmacol* **62**:627-633.
- Bijsterbosch MK, Rump ET, De Vruhe RL, Dorland R, van Veghel R, Tivel KL, Biessen EA, van Berkel TJ, and Manoharan M (2000) Modulation of plasma protein binding and in vivo liver cell uptake of phosphorothioate oligodeoxynucleotides by cholesterol conjugation. *Nucleic Acids Res* **28**:2717-2725.
- Boutorine AS and Kostina EV (1993) Reversible covalent attachment of cholesterol to oligodeoxyribonucleotides for studies of the mechanisms of their penetration into eucaryotic cells. *Biochimie* **75**:35-41.
- Brenner DA, Rippe RA, Rhodes K, Trotter JF, and Breindl M (1994) Fibrogenesis and type I collagen gene regulation. *J Lab Clin Med* **124**:755-760.
- Cheng K, Ye Z, Guntaka RV, and Mahato R (2005) Biodistribution and hepatic uptake of triplex-forming oligonucleotides against type alpha1(I) collagen gene promoter in normal and fibrotic rats. *Mol Pharm* **2**:206-217.
- Crooke ST, Graham MJ, Zuckerman JE, Brooks D, Conklin BS, Cummins LL, Greig MJ, Guinasso CJ, Kornbrust D, Manoharan M, et al. (1996) Pharmacokinetic properties of several novel oligonucleotide analogs in mice. *J Pharmacol Exp Ther* **277**:923-937.
- Feener EP, Shen WC, and Ryser HJ (1990) Cleavage of disulfide bonds in endocytosed macromolecules: a processing not associated with lysosomes or endosomes. *J Biol Chem* **265**:18780-18785.
- Friedman SL (2000) Molecular regulation of hepatic fibrosis, an integrated cellular response to tissue injury. *J Biol Chem* **275**:2247-2250.
- Godard G, Boutorine AS, Saison-Behmoaras E, and Helene C (1995) Antisense

- effects of cholesterol-oligodeoxynucleotide conjugates associated with poly(alkylcyanoacrylate) nanoparticles. *Eur J Biochem* **232**:404–410.
- Holasova S, Mojzisek M, Buncek M, Vokurkova D, Radilova H, Safarova M, Cervinka M, and Haluza R (2005) Cholesterol conjugated oligonucleotide and LNA: a comparison of cellular and nuclear uptake by Hep2 cells enhanced by streptolysin-O. *Mol Cell Biochem* **276**:61–69.
- Inagaki Y, Truter S, Greenwel P, Rojkind M, Unoura M, Kobayashi K, and Ramirez F (1995) Regulation of the alpha 2(I) collagen gene transcription in fat-storing cells derived from a cirrhotic liver. *Hepatology* **22**:573–579.
- Jamall IS, Finelli VN, and Que Hee SS (1981) A simple method to determine nanogram levels of 4-hydroxyproline in biological tissues. *Anal Biochem* **112**:70–75.
- Jenkins SA, Grandison A, Baxter JN, Day DW, Taylor I, and Shields R (1985) A dimethylnitrosamine-induced model of cirrhosis and portal hypertension in the rat. *J Hepatol* **1**:489–499.
- Jezequel AM, Mancini R, Rinaldesi ML, Macarri G, Venturini C, and Orlandi F (1987) A morphological study of the early stages of hepatic fibrosis induced by low doses of dimethylnitrosamine in the rat. *J Hepatol* **5**:174–181.
- Joseph J, Kandala JC, Veerapanane D, Weber KT, and Guntaka RV (1997) Antiparallel polypurine phosphorothioate oligonucleotides form stable triplexes with the rat alpha1(I) collagen gene promoter and inhibit transcription in cultured rat fibroblasts. *Nucleic Acids Res* **25**:2182–2188.
- Juliano RL, Alahari S, Yoo H, Kole R, and Cho M (1999) Antisense pharmacodynamics: critical issues in the transport and delivery of antisense oligonucleotides. *Pharm Res (NY)* **16**:494–502.
- Knittel T, Kobold D, Saile B, Grundmann A, Neubauer K, Piscaglia F, and Ramadori G (1999) Rat liver myofibroblasts and hepatic stellate cells: different cell populations of the fibroblast lineage with fibrogenic potential. *Gastroenterology* **117**:1205–1221.
- Krieg AM, Tonkinson J, Matson S, Zhao Q, Saxon M, Zhang LM, Bhanja U, Yakubov L, and Stein CA (1993) Modification of antisense phosphodiester oligodeoxynucleotides by a 5' cholesteryl moiety increases cellular association and improves efficacy. *Proc Natl Acad Sci USA* **90**:1048–1052.
- MacKellar C, Graham D, Will DW, Burgess S, and Brown T (1992) Synthesis and physical properties of anti-HIV antisense oligonucleotides bearing terminal lipophilic groups. *Nucleic Acids Res* **20**:3411–3417.
- Manoharan M (2004) RNA interference and chemically modified small interfering RNAs. *Curr Opin Chem Biol* **8**:570–579.
- Nakanishi M, Weber KT, and Guntaka RV (1998) Triple helix formation with the promoter of human alpha1(I) procollagen gene by an antiparallel triplex-forming oligodeoxyribonucleotide. *Nucleic Acids Res* **26**:5218–5222.
- Oberhauser B and Wagner E (1992) Effective incorporation of 2'-O-methyl-oligoribonucleotides into liposomes and enhanced cell association through modification with thiocholesterol. *Nucleic Acids Res* **20**:533–538.
- Okamoto H, Kato N, Iizuka H, Tsuda F, Miyakawa Y, and Mayumi M (1999) Distinct genotypes of a nonenveloped DNA virus associated with posttransfusion non-A to G hepatitis (TT virus) in plasma and peripheral blood mononuclear cells. *J Med Virol* **57**:252–258.
- Pfaffl MW (2001) A new mathematical model for relative quantification in real-time RT-PCR. *Nucleic Acids Res* **29**:e45.
- Sato M, Suzuki S, and Senoo H (2003) Hepatic stellate cells: unique characteristics in cell biology and phenotype. *Cell Struct Funct* **28**:105–112.
- Simons K and Ikonen E (2000) How cells handle cholesterol. *Science (Wash DC)* **290**:1721–1726.
- Wang L, Kristensen J, and Ruffner DE (1998) Delivery of antisense oligonucleotides using HPMA polymer: synthesis of A thiol polymer and its conjugation to water-soluble molecules. *Bioconjug Chem* **9**:749–757.
- Ye Z, Cheng K, Guntaka RV, and Mahato RI (2005) Targeted delivery of a triplex-forming oligonucleotide to hepatic stellate cells. *Biochemistry* **44**:4466–4476.
- Zhang Z, Zhang T, and Zhang Q (1997) The push-pull theory of migration and its application. *Chin J Popul Sci* **9**:255–263.

Address correspondence to: Dr. Ram I. Mahato, University of Tennessee Health Science Center, Department of Pharmaceutical Sciences, 26 South Dunlap Street, Feurt 413, Memphis, TN 38163. E-mail: rmahato@utm.edu
